

GENERATING DIGITAL TERRAIN MODELS USING LROC NAC IMAGES

T. Tran^a, M. R. Rosiek^b, Ross A. Beyer^{cd}, S. Mattson^e, E. Howington-Kraus^b, M.S. Robinson^a, B. A. Archinal^b, K. Edmundson^b, D. Harbour^b, E. Anderson^a, and the LROC Science Team

^aArizona State University, School of Earth and Space Exploration, 1100 S Cady, Tempe AZ, 85287 – (thanh.n.tran@asu.edu)

^bUnited States Geological Survey, Astrogeology Science Center, 2255 N Gemini Dr, Flagstaff AZ. 86001 –(mrosiek, ahowington, barchinal, kedmundson)@usgs.gov

^cCarl Sagan Center at the SETI Institute; ^dNASA Ames Research Center, Mail Stop 245-3 (Bldg. N245), Moffett Field, CA, USA (Ross.A.Beyer@nasa.gov);

^eUniversity of Arizona, Lunar and Planetary Lab, Tucson, AZ 85721

Commission VI, WG VI/4

KEY WORDS: DTM, LROC, topography, Moon, mapping

ABSTRACT:

The Lunar Reconnaissance Orbiter Camera (LROC) consists of one Wide Angle Camera (WAC) for synoptic multispectral imaging and two Narrow Angle Cameras (NAC) to provide high-resolution images (0.5 to 2.0 m pixel scale) of key targets. LROC was not designed as a stereo system, but can obtain stereo pairs through images acquired from two orbits (with at least one off-nadir slew). Off-nadir rolls interfere with the data collection of the other instruments, so during the nominal mission LROC slew opportunities are limited to three per day.

This work describes a methodology of DTM generation from LROC stereo pairs and provides a preliminary error analysis of those results. DTMs are important data products that can be used to analyze the terrain and surface of the Moon for scientific and engineering purposes. As of 12 September 2010, we have processed 30 NAC stereo pairs to DTMs with absolute control to the Lunar Orbiter Laser Altimeter (LOLA) dataset. For the high-resolution stereo images (~0.5 mpp) from the primary phase, the DTM vertical precision error and the elevation fitting error to the LOLA data is expected to be less than 1 meter. For the lower resolution stereo images (~1.5 mpp) from the commissioning phase, the vertical precision error and elevation fitting error is expected to be 3 meters. This does not include an estimate of absolute error at this time. This will be included when the final LOLA data is available. There are six independent groups generating DTMs (ASU, DLR/TUB, UA, USGS, OSU, and Ames), and collaboration will result in a detailed error analysis that will allow us to fully understand the capabilities of the DTMs made from LROC datasets.

1. INTRODUCTION

1.1 LROC NAC

The Lunar Reconnaissance Orbiter is currently in operation around the Moon (Chin et al. 2007, Vondrak et al, 2010). Two instruments on board the spacecraft enable the extraction of digital terrain models (DTMs): Lunar Reconnaissance Orbiter Camera (LROC) and Lunar Orbiter Laser Altimeter (LOLA.) LROC consists of one Wide Angle Camera (WAC) for synoptic multispectral imaging, and two Narrow Angle Cameras (NAC) to provide high-resolution images (0.5 to 1.5 m pixel scale) of key targets (Robinson et al. 2010a, 2010b.) LROC was not designed as a stereo system, but can obtain stereo pairs through images acquired from two orbits (with at least one off-nadir slew). Typically the two observations that form a geometric stereo pair have different slew angles ranging from zero to twenty degrees (Beyer et al. 2009). To obtain an accurate DTM, the convergence angle between the two images should be more than 12° for images with a 0.5 pixel scale (Cook et al. 1996). Off-nadir rolls interfere with the data collection of the other instruments, so during the LRO Exploration Systems Mission Directorate primary phase LROC slew opportunities are limited to three per day on average (Robinson et al. 2010b).

1.2 LOLA

LOLA is designed to assess the shape of the Moon by measuring precisely the range from the spacecraft to the lunar surface, incorporating precision orbit determination of LRO and referencing surface ranges to the Moon's center of mass. LOLA has 5 beams and operates at 28 Hz, with a nominal accuracy of 10 cm. One of its primary objective is to produce a global geodetic grid for the Moon to which all other observations can be precisely referenced (Smith et al. 2010, Zuber et al. 2010.)

1.3 DTM Collection

The LROC team has representatives from six different groups using four different methods to create DTMs.

1. Arizona State University (ASU)
2. German Aerospace Center (DLR), Institute of Planetary Research and Technical University Berlin (TUB)
3. NASA Ames Research Center (Ames)
4. University of Arizona (UA)
5. Ohio State University (OSU)
6. United States Geological Survey (USGS)

ASU, NASA Ames, UA, and USGS all use SOCET SET (DeVenecia et al. 2007) for photogrammetric processing the NAC images, while OSU uses Orbital Mapper and Leica Photogrammetry Suite 9.3. DLR/TUB uses photogrammetry software developed in-house. In addition, NASA Ames is using the NASA Ames Stereo Pipeline, also developed in-house. All of these groups have successfully processed LROC images to high precision DTMs. Models have been made of 30 locales, including the Apollo 15, 16, and 17 landing sites, as they contain useful landmarks for absolute positioning (Davies and Colvin, 2000, Archinal et al. 2010, Oberst et al. 2010), are of operational and scientific interest as ground truth sites, and are of general interest due to their historical importance (Beyer et al. 2010).

Analysis by six groups using four techniques on similar data allows an important initial comparison of derived camera parameters and an assessment of LROC DTM quality. Deriving DTMs of areas that include positioning landmarks (Archinal et al. 2010) allows us to tie together LRO and other lunar datasets, and to assist the Lunar Mapping and Modelling Project (LMMP) (Noble et al. 2009) in deriving DTMs and controlled mosaics of the Constellation Program regions of interest (Gruener and Joosten, 2009).

The objective of this paper is to (i) describe the methodology of DTM generation from LROC NAC stereo pairs based on the method being used by ASU, UA, USGS, and NASA Ames and (ii) to discuss preliminary error analysis on the results.

2. DATA SOURCES

2.1 LROC NAC

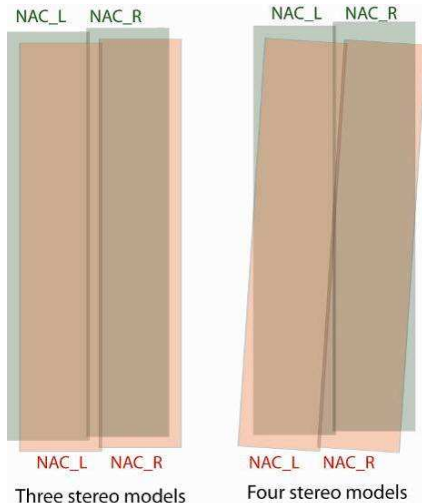


Figure 1. Stereo Models

The LROC NACs are linear pushbroom cameras built using the Kodak KLI-5001G line array. The line array is a 5064 element CCD with 7-micron pixels. The two NAC cameras are designated NAC-Left (NAC_L) and NAC-Right (NAC_R) and these names are reflected in the image filename with NAC_L images having an L in the filename and NAC_R images having an R in the filename. Each camera is designed to provide 0.5 m resolution panchromatic images covering a 2,500 m swath width, for a combined coverage of 5,000 m, at an altitude of 50

km. Each camera has an internal buffer of 256 MB; allowing for image length of 52,224 lines or 26,112 m. The NAC images are sampled at 12 bits, and companded to 8 bits. Each camera has its own optics, and they are aligned to overlap by ~135 pixels in the cross-track direction and are offset from each other by ~185 pixels in the down-track direction (Robinson et al. 2010b).

Stereo images are collected by acquiring images on two different orbits so the total parallax angle is greater than 12°. On average the parallax angle is about 24°. The overlap between the two NAC_L and NAC_R images provides three or four stereo models from which to collect elevation data. The number of models depends on whether the areas where the right and left images overlap are parallel or intersect each other (Figure 1). The amount of overlap and the actual footprint are affected by the topography and the orbit parameters (target center point, latitude, and slew angle).

2.2 LOLA

LOLA is a pulse detection time-of-flight altimeter that incorporates a five-spot pattern to measure the precise distance to the lunar surface at 5 spots simultaneously, thus providing 5 profiles across the lunar surface for each orbit. LOLA fires at a fixed, 28-Hz rate, so that for a nominal 1600 m/s ground track speed there is one shot approximately every 57 m. At a nominal 50-km altitude, each spot within the five-spot pattern has a diameter of 5 m while each detector field of view has a diameter of 20 m. The spots are 25 meters apart, and form a cross pattern canted by 26 degrees counterclockwise to provide five adjacent profiles (PDS Geoscience Node 2010, Smith et al. 2010, Zuber et al. 2010.) The LOLA instrument boresight is aligned with the LROC NAC cameras to enable altimetry data collection in the overlap region between the NAC_L and NAC_R.

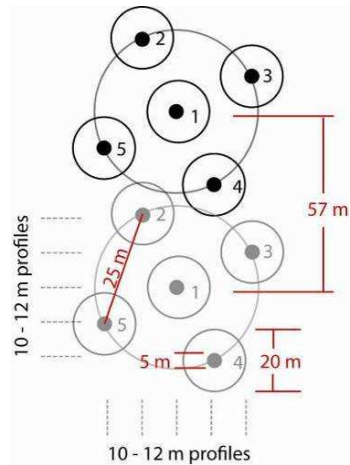


Figure 2 - LOLA spot pattern

Tracking of LRO is currently within 10 m radial and 300 m horizontal accuracy (Zuber et al. 2010.) By using Earth-based laser ranging tracking and crossover analysis, the expected accuracy of the LOLA data will be 1 m radial and 50 m horizontal.

3. METHODOLOGY

To generate the DTMs, we use a combination of the USGS Integrated Software for Imagers and Spectrometers (ISIS) (see

<http://isis.astrogeology.usgs.gov/>) and SOCET SET® from BAE Systems. ISIS routines ingest the image files, perform a radiometric correction, and export to a format SOCET SET accepts. The NAC files imported into SOCET SET are Level 1 radiometrically corrected images and a list of keywords of relevant parameters, such as spacecraft coordinates, altitude, Euler angles, and ephemeris positions.

SOCET SET uses a generic pushbroom sensor model to relate the image space to ground coordinates. Often times, there is a bias error in the camera pointing, which we correct with multi-sensor triangulation (MST), more commonly known as bundle adjustment, to update the parameters (position, velocity, pointing angles, etc.) to improve the registration between overlapping images and between images and ground truth. MST performs an aero-triangulation using sensor position, sensor pointing, ground points, and image tie points. Ground points tie a point or identifiable object in the image to a point on the ground, and tie points relate a point in the overlap regions of two or more images. Selected parameters, such as the position, velocity, and pointing angles are adjusted so that the residual RMS for all ground and tie point measurements is minimized. When working with a pair of LROC NAC stereo images, the RMS residuals are typically ~0.25 pixels and are rarely larger than 0.4 pixels. When working with multiple sets of stereo images of the same region, there may be points with larger residuals, but the overall solution is typically under 1 pixel.

Once MST completes with an acceptable residual RMS, the process of extracting DTMs can begin with NGATE (SOCET SET – Next Generation Automatic Terrain Extraction). NGATE performs image correlation and edge matching for every single pixel in the image to create a dense model. The result is then re-sampled to the desired DTM resolution (meters/post) that can be anywhere between 3 to 10 times the pixel scale of the image to minimize noise. For images with moderate Sun (35°-65° incidence angle), results from NGATE require very little editing. However, images with areas of instrument saturation or low Sun (large shadowed regions), and areas of high Sun where albedo dominate morphological features require intensive editing and interpolating across areas of no ground data.

NGATE is not optimized to work with linear pushbroom images. One way to increase the effectiveness is to perform a pair-wise rectification on the images that will be used in the DTM extraction. This process rotates the images so that the epipolar lines are horizontal and scales the images to a common pixel scale. The rectified images make stereo vision easier on the eyes and are required for accurate generation of the DTM. Another way to increase the effectiveness is to generate a continuous rational polynomial sensor model for the images. The advantage of this method is that if pair-wise rectification is used then 3 or 4 sets of images would need to be generated (NAC_L – NAC_L, NAC_R – NAC_R, NAC_L – NAC_R, NAC_R – NAC_L) depending on how many stereo models are formed by the LROC NAC images (Figure 1.) The continuous rational polynomial sensor model images can be combined with different images since they are generated independent of any other image.

Our standard products include the DTM and orthorectified images in ISIS cube format. In addition, a hillshade image, color shaded relief image, slope map, and confidence map are provided in GeoTIFF format. These products will be made

available to the science community when error analysis and documentation is complete.

4. ERROR ANALYSIS

The quality of a DTM is measured as a combination of absolute accuracy (latitude, longitude, and elevation at each pixel) and relative accuracy (relative relief and slopes internal to the DTM). The LOLA data will be used to define the geodetic reference frame for the DTMs extracted from the images. After a final crossover analysis is performed on the LOLA data and it is adjusted to be self consistent, the adjusted data can then serve as the best possible absolute accuracy geodetic reference frame to which the DTMs can be referenced. This section will focus on the relative accuracy analysis of the DTMs and how well the DTMs are matched (referenced) to the LOLA elevation values. The match between the LOLA elevation values and DTMs will improve as errors in the LOLA data are reduced.

4.1 Expected Vertical Precision

Based on the spacecraft orbit and camera geometry, the theoretical expected vertical precision can be calculated. During the nominal mission, LRO is in a 50 km circular orbit. During image acquisition, LRO is either pointed nadir or rotated about the flight line (normal situation) to acquire a stereomate. In some cases, LRO can also be pitched forward to acquire stereo images in the polar regions. The convergence angle is the total parallax angle between the two stereo pairs. Based on the spacecraft geometry, we can calculate the expected vertical precision using base to height ratio, assuming the instantaneous field of view (IFOV) or ground sample distance (GSD) of 0.5 m, and feature match RMS error of 0.2 pixels (Cook et al. 1996.). Figure 3 shows the expected vertical precision for convergence angle between 5 and 40 degrees.

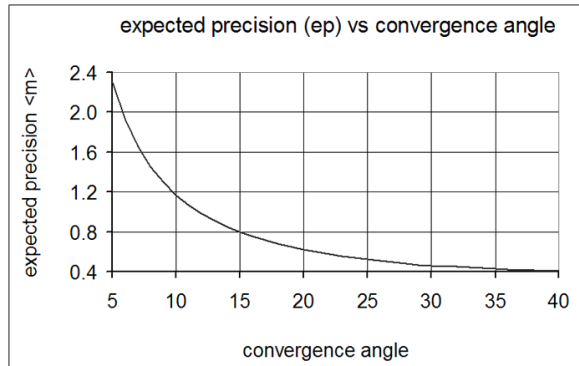


Figure 3 - Expected precision

4.2 Spacecraft Jitter

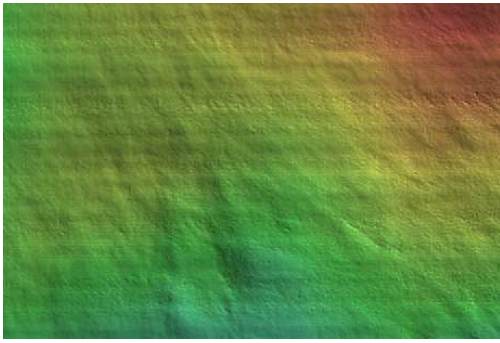


Figure 4 - Jitter in the Giordano Bruno DTM.

Spacecraft induced jitter during stereo image acquisition results in artificial topographic ripples in some NAC DTMs (Mattson et al. 2010.) We see these artifacts in about 10% of stereo models taken during the LRO commissioning phase. The LROC Team and the LRO project are working to determine the cause of the jitter and to mitigate the problem in the mapping phase of the mission (Mattson et al. 2010), and so far no jitter has been detected in the ESMD primary mission. The artificial ripples are readily apparent in derived shaded relief products with illumination along the down-track direction. For the Giordano Bruno DTM (Figure 4), jitter is seen as consistent banding in the cross-track direction, with higher frequency bands occurring every ~200 meters and lower frequency bands occurring every ~800 meters.

Most images do not have jitter and result in excellent DTMs. Shown in Figure 5 is a subset of the color hill shaded mosaic for Lichtenberg crater. The entire DTM is based on 8 LRO NAC image pairs.

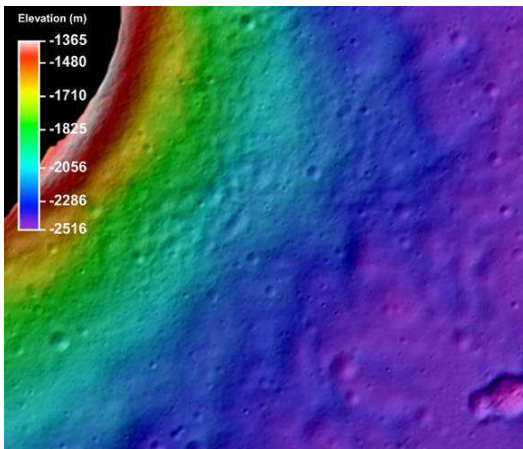


Figure 5 - Color hill shade of Lichtenberg crater

4.3 Error between DTM and LOLA

There are different methods for connecting the image location with the elevation values in the LOLA profiles, so the error analysis differs.

4.3.1 Method 1: Matching based on geomorphic features

One method is to use geomorphic features that can be identified in the images and the LOLA profiles. Bottoms of craters, tops of hills, and breaks-in-grade can be matched between the stereo images and the LOLA profiles. This method was used for absolute control at the Apollo 15 site. The initial comparison between an unedited DTM and the LOLA profiles showed that the difference between LOLA and DTM elevation values ranged from -88 to 245 m. By eliminating errors below -35 m and above 30 m, only 55 out of 2,199 LOLA points were eliminated from orbit 1576. These outliers will have to be investigated to determine if the error is in the DTM or the LOLA observations. By eliminating these high-error points the range in difference values has a minimum of -34.7 and a maximum of 25.6 m.

Table 1 – preliminary error analysis – Method 1

Orbit	# Points	Average Error (m)	Std Dev Error (m)	RMS Error (m)
3060	1,613	1.4	1.7	2.2
1229	1,722	2.9	1.6	3.4
2792	1,762	-3.1	2.0	3.7
1577	2,212	-2.8	3.3	4.3
1924	2,447	3.6	3.7	5.1
2887	981	7.4	5.8	9.4
*1576	2,144	8.7	4.2	9.7
2445	2,195	10.1	4.4	11.1
2793	2,441	14.0	1.1	14.0
ALL	17,517	4.9	6.6	8.3

* 55 points were eliminated from this orbit

Our preliminary vertical accuracy analysis for a DTM of the Apollo 15 site is summarized in Table 1. The Apollo 15 DTM has a pixel scale of 1.5 m generated from images with a pixel scale of 0.5 m. For the bundle adjustment, there are 9 pairs of LROC NAC images (18 NAC_L and NAC_R images) and 18 geomorphic points were picked to tie the images to the LOLA elevation points. The NAC DTM is on average within 5 m for five of the nine LOLA profiles (9,756 points). Since this DTM is part of a larger bundle block adjustment, the other DTMs will need to be examined to determine if a commensurate error applies to other DTMs. The RMS errors for all the orbits are comparable to the RMS errors reported in Table 2.

After registering the LOLA profiles and the DTM, the two datasets were differenced and the residual is plotted as the cumulative percent of points in the profile (Figure 5). The profiles were ordered from lowest to highest RMSE. Orbits 2792, 2793, and 3060 are relatively flat lines with small tails and have the lowest standard deviations shown in Table 1. The time difference between sequential orbits (1576 and 1577, and 2792 and 2793) is about 2 hours, and it's interesting to note that the error between the LOLA and DTM elevation values for sequential orbits do not differ from the other orbits. The plotted lines show that the DTM is on average lower than LOLA elevations.

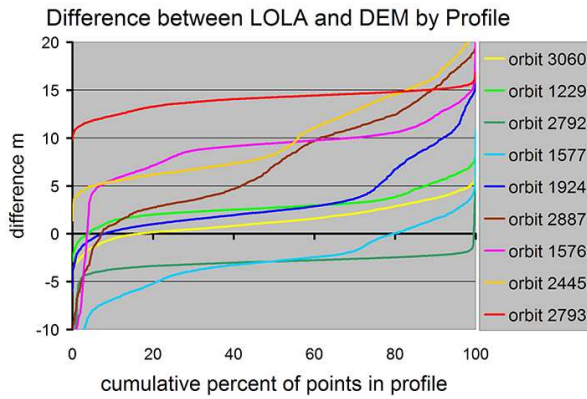


Figure 6 - LOLA profile plot

The LOLA vs DTM difference was overplotted on a NAC DTM derived shaded relief map to reveal systematic errors (Figure 6). The area north of 26° latitude is a plain about -2100 m in elevation. South of 26° is the beginning of Mons Hadley, rising 3300 m above the plain. Within the flat region in the plain, most of the absolute errors are less than 10 m and the majority of the errors are below 2 m. The errors are systematic and correlated within each profile. There is not any tilt apparent in the DTM relative to the LOLA points. This correlation shows that the DTM has been leveled with respect to the LOLA data. In the Mons Hadley region the absolute errors have more variation indicating the possibility of a spatial offset between the LOLA profiles and the DTM. After the LOLA profiles are corrected with the crossover analysis, these errors should be reduced. The DTM was not edited so some blunders in the DTM account for some of the large errors.

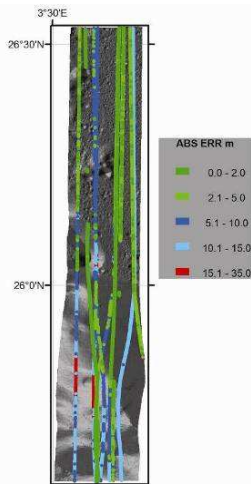


Figure 6 - Difference between LOLA and DTM

4.3.2 Method 2: Matching based on aligning a profile

Another method to match the DTM to the LOLA profiles is to use software capable of 3D plotting to allow visual rotation of the DTM and LOLA data. The current version of SOCET SET has a powerful graphical interface that allows users to visualize the depth of the stereo model, however, visualizing the depth only gives a qualitative perspective and not a quantitative perspective needed for precise placement of the LOLA profiles. Within SOCET SET, one can only display images from the

orthogonal direction, but in other packages (i.e. MATLAB, ENVI, etc.), one can visualize both the LOLA profiles and the DTM in a 3-dimensional state. This vantage point allows users to know exactly where to place the geomorphic points so the profiles and the DTM line up more accurately. Additionally, we use MATLAB to perform autocorrelation between the placement of the LOLA profile within the DTM and determine which placement has the lowest error. The algorithm that we currently use is in its early stages of development, and it considers simultaneously changing 6 parameters: displacement in the longitude (X), latitude (Y), and elevation (Z) direction, rotation about the X and Z-axis, and scaling in the Y direction. The result of this script is the image location of the control points and the corresponding latitude, longitude, and elevation.

The advantage of using the MATLAB script is it removes ambiguity associated with the locations (image sample and line) of the geomorphic points. However, this technique is more time consuming because it requires the user to extract and edit the DTM of an area overlapping the profile of interest before they can be imported into MATLAB. Currently, the LOLA profiles are inconsistent with each other, so our strategy is to tie the DTM as best as we can with the help of MATLAB to one profile, which we called the primary profile. This ensures that the model is fixed in the down-track direction (Figure 7). The other profiles (secondary profiles) are then used to tie the elevation of the model to control the possible tilt about the primary profile (Figure 8). If the secondary profiles have a spatial and elevation offset from the primary profile, then the error in the slope of the DTM could be up to 1° in the cross-track direction.

Table 2 -- Preliminary Error Analysis – Method 2

Locations	Col. A	Col. B	Col. C
Aristarchus Plateau 1 (2 mpp*)	0.42	0.84	14.36
Gruithuisen Domes (2 mpp)	0.77	0.91	--
Ina D-Caldera (2 mpp)	0.43	1.20	10.46
Lichtenberg Crater (2 mpp)	0.48	1.04	5.23
South-Pole Aitken (2 mpp)	1.19	1.41	19.63
Hortensius Domes (5 mpp)	2.42	2.18	9.46
Marius Hills (5 mpp)	5.70	2.27	8.33
Reiner Gamma (5 mpp)	4.98	3.56	7.66
Sulpicius Gallus (5 mpp)	3.08	3.06	10.22

* meters per post (mpp)

The 2mpp DTMs are from high-resolution nominal phase stereo images, and the 5mpp DTMs are from lower resolution commissioning phase images (Table 2). The errors from commissioning phase DTMs are higher than the errors from nominal phase DTMs due to the limits of resolution.

- Column A shows the precision error (m) reported in the DTM header file generated by SOCET SET.
- Column B shows the RMS error (m) between the primary LOLA profile and the DTM. This error provides insight on how well the DTM and LOLA data agree.
- Column C shows the RMS error (m) between all of the LOLA profiles that overlap the DTM and the DTM. Because the LOLA profiles have not been adjusted using a crossover analysis, this error is dominated by the spatial and elevation offset between different LOLA data profiles.

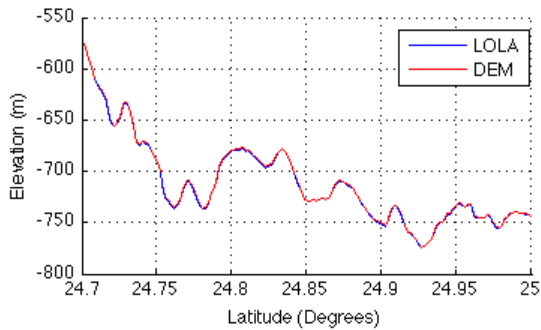


Figure 7. Main profile from Aristarchus region (longitude $\sim 48.68^\circ$). The RMS error is 0.75 meters.

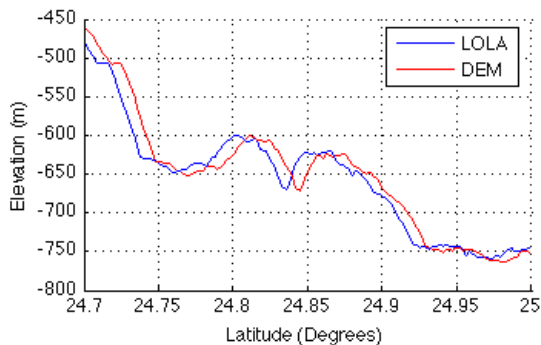


Figure 8. Secondary profile from Aristarchus region (longitude $\sim 48.81^\circ$). The RMS error is 18.94 meters. The high magnitude of the error reflects the spatial offset between the LOLA data and the DTM most likely due to uncertainties in the current LRO ephemeris.

5. PRELIMINARY ERROR ANALYSIS SUMMARY

The absolute horizontal and vertical accuracy of the DTM largely depends on the absolute horizontal and vertical accuracy of the LOLA data. The relative horizontal accuracy (pixel to pixel across the DTM) is the same as the spatial resolution of the DTM. The absolute horizontal accuracy is the absolute horizontal accuracy of the LOLA data. As of 12 September 2010, the absolute horizontal accuracy of the LOLA data can be up to 300 meters. It is expected that the absolute horizontal accuracy of the LOLA data be as low as 50 meters with the crossover analysis.

The vertical accuracy of the DTM is limited by both the absolute vertical accuracy of the LOLA data and the Expected Vertical Precision (the relative precision) of the DTM. The absolute vertical accuracy of the LOLA data is expected to approach 1 meter, but as of 12 September 2010, the vertical accuracy of the LOLA data is approximately 10 meters. The relative precision of the DTM from nominal phase is expected to be 0.5 meters, but can be as large as 1.5 meters. The relative precision of the DTM from commissioning phase is expected to be 3 m.

Each technique used to match the DTM to the LOLA dataset has merit. The first technique uses geomorphic points from all profiles, so the final bundle adjustment solution has least square error from all profiles. Because of discrepancies between the LOLA profiles, there is a possibility of a slope error in both the down-track and cross-track direction. The second technique

uses geomorphic points from one primary profile and elevation control points from all other profiles. The slope error in the down-track direction should be close to 0° because the RMS error along the primary track is typically less than 1 m. However, because of potential spatial and elevation offset from secondary profiles, the slope in the cross-track direction can have an error of up to 1° .

6. FUTURE WORK

NAC derived DTMs, along with the data from other sensors onboard LRO, will be an important contribution to science analysis. Therefore, it is important that the DTMs portray terrain as detailed and accurate as possible. Several ideas that we plan to implement include: (i) compare the DTMs of one site made using two different datasets, (ii) compare the DTMs that we made with DTMs that other groups made whether they use the same technique or different technique, and (iii) compare the DTMs with DTMs derived from Apollo era photographs. The successful completion of these tasks will allow us to fully understand the capabilities of the DTMs made from LROC datasets.

For the LMMP mapping tasks, the DTMs that are generated will be adjusted to be the final LOLA data after the LOLA data is adjusted with a crossover analysis. This work is expected to be completed in September 2011.

7. ACKNOWLEDGEMENTS

Thanks to the LROC and LOLA Science Operations Center Team, and the LRO Mission Management Team for all the hard work and dedication to acquire the stereo images and altimetry data. Thanks to LMMP for support of map making.

8. REFERENCES

- Archinal, B.A., Duxbury, T.C., Scholten, F., Oberst, J., Danton, J., Robinson, M.S., Smith, D.E., Neumann, G.A., Zuber, M., LROC Team, LOLA Team, 2010. Tying LRO Data to the Fundamental Lunar Laser Ranging Reference Frame. 41st Lunar and Planetary Science Conference, Houston TX, March 2010, Abs. #2609.
- Beyer, R.A., Archinal, B., Li, R., Mattson, S., McEwen, A., Robinson, M.S., 2009. LROC Stereo Observations. LROC Science Targeting Meeting, Tempe AZ 2009, LPI Cont. 1483, pp.15-16.
- Beyer, R.A., Archinal, B., Chen, Y., Edmundson, K., Harbour, D., Howington-Kraus, E., Li, R., McEwen, A., Mattson, S., Moratto, Z., Oberst, J., Rosiek, M., Scholten, F., Tran, T., Robinson, M., LROC Team, 2010. LROC Stereo Data — Results of Initial Analysis. 41st Lunar and Planetary Science Conference, Houston TX, March 2010, Abs. #2678.
- Chin, G., Brylow, S., Foote, M., Garvin, J., Kasper, J., Keller, J., Litvak, M., Mitrofanov, I., Paige, D., Raney, K., et al., 2007. Lunar Reconnaissance Orbiter Overview: The Instrument Suite and Mission. *Space Sci Rev* (2007) 129:391–419, DOI: 10.1007/s11214-007-9153-y
- Cook, A.C., Oberst, J., Roatsch, T., Jaumann, R., Acton, C., 1996. Clementine Imagery: Selenographic Coverage for Cartographic and Scientific use. *Planetary and Space Science*,

Volume 44, Issue 10, October 1996, Pages 1135-1148, ISSN 0032-0633, DOI: 10.1016/S0032-0633(96)00061-X.

Davies, M.E., Colvin, T. R., 2000. Lunar coordinates in the regions of the Apollo Landers. *Journal of Geophysical Research*, Volume 105, Issue E8, 20,277–20,280, DOI: 10.1029/1999JE001165

DeVenecia, K., Walker, A.S., Zhang, B., 2007. New approaches to generating and processing high resolution elevation data with imagery. *Photogrammetric Week 2007*, edited by D. Fritsch, pp. 297–308, Wichmann, Heidelberg.

Gruener, J.E., Joosten, B.K., 2009. NASA Constellation Program Office Regions of Interest on the Moon: A Representative Basis for Scientific Exploration, Resource Potential, and Mission Operations. Lunar Reconnaissance Orbiter Science Targeting Meeting, Tempe, AZ June 9-11, 2009, Abstract #6036

Mattson, S., Robinson, M., McEwen, A., Bartels, A., Bowman-Cisneros, E., Li, R., Lawver, J., Tran, T., Paris, K., LROC Team, 2010. Early Assessment of Spacecraft Jitter in LROC-NAC. 41st Lunar and Planetary Science Conference, Houston TX, March 2010, Abs. #1871.

Noble, S.K., French, R.A., Nall, M.E., K. G., 2009. The Lunar Mapping and Modeling Project. Houston TX Nov. 16-19, 2009 Annual Meeting of Lunar Exploration Analysis Group #2014

Oberst, J., Scholten, F., Matz, K.D., Roatsch, T., Wählisch, M., Haase, I., Gläser, P., Gwinner, K., Robinson, M.S., LROC Team, 2010. Apollo 17 Landing Site Topography from LROC NAC Stereo Data - First Analysis and Results. 41st Lunar and Planetary Science Conference, Houston TX, March 2010, Abs. #2051.

PDS Geosciences Node, 2010. LOLA RDR Query Page (Moon ODE), Washington University in St. Louis, <http://ode.rsl.wustl.edu/mars/pagehelp/quickstartguide/lolardquery.htm> (accessed 6 Sep. 2010)

Robinson M.S., Eliason, E.M., Hiesinger, H., Jolliff, B.L., McEwen, A.S., Malin, M.C., Ravine, M.A., Thomas, P.C., Turtle, E.P., Bowman-Cisneros, E., LROC Team, 2010a. Lunar Reconnaissance Orbiter Camera: First Results. 41st Lunar and Planetary Science Conference, Houston TX, March 2010, Abs. #1874.

Robinson, M.S., Brylow, S.M., Tschimmel, M., Humm, D., Lawrence, S.J., Thomas, P.C., Denevi, B.W., Bowman-Cisneros, E., Zerr, J., Ravine, M.A., Caplinger, M.A., Ghaemi, F.T., Schaffner, J.A., Malin, M.C., Mahanti, P., Bartels, A., Anderson, J., Tran, T.N., Eliason, E.M., McEwen, A.S., Turtle, E., Jolliff, B.L., Hiesinger, H., 2010b. Lunar Reconnaissance Orbiter Camera (LROC) Instrument Overview. *Space Sci Rev* (2010) 150: 81–124 DOI 10.1007/s11214-010-9634-2

Smith, D.E., Zuber, M., Jackson, G.B., Cavanaugh, J.F., Neumann, G.A., Riris, H., Sun, X., Zellar, R.S., Coltharp, C., Connelly, J., Katz, R.B., Kleyner, I., Liiva, P., Matuszeski, A., Mazarico, E.M., McGarry, J.F., Novo-Gradac, A., Ott, M.N., Peters, C., Ramos-Izquierdo, L.A., Ramsey, L., Rowlands, D.D., Schmidt, S., Scott, V.S., Shaw, G.B., Smith, J.C., Swinski, J.P., Torrence, M.H., Unger, G., Yu, A.W.,

Zagwodzki, T.W., 2010. The Lunar Orbiter Laser Altimeter Investigation on the Lunar Reconnaissance Orbiter Mission. *Space Sci Rev* (2010) 150: 209–241 DOI 10.1007/s11214-009-9512-y

Vondrak, R., Keller, J., Chin, G., Garvin, J., 2010. Lunar Reconnaissance Orbiter (LRO): Observations for Lunar Exploration and Science. *Space Sci Rev* (2010) 150: 7–22 DOI 10.1007/s11214-010-9631-5

Zuber, M.T., Smith, D.E., Zellar, R.S., Neumann, G.A., Sun, X., Katz, R.B., Kleyner, I., Matuszeski, A., McGarry, J.F., Ott, M.N., Ramos-Izquierdo, L., Rowlands, D., Torrence, M.H., Zagwodzki, T.W., 2010. The Lunar Reconnaissance Orbiter Laser Ranging Investigation. *Space Sci Rev* (2010) 150: 63–80 DOI 10.1007/s11214-009-9511-z